

Semidefinite Programming Relaxation Based Virtually Antipodal Detection for MIMO Systems Using Gray-Coded High-Order QAM

Shaoshi Yang, *Student Member, IEEE*, Tiejun Lv, *Senior Member, IEEE*,
and Lajos Hanzo, *Fellow, IEEE*

Abstract—An efficient generalized semidefinite programming relaxation (SDPR) based virtually antipodal (VA) detection approach is proposed for Gray-coded high-order rectangular quadrature amplitude modulation (QAM) signalling over multiple-input-multiple-output (MIMO) channels. Albeit the decomposition of symbol-based detection to a bit-based one is desirable owing to its reduced complexity and increased flexibility, Gray-mapping is nonlinear, and hence the direct bit-based detection of Gray-coded-QAM MIMO systems constitutes a challenging problem. In this paper, we find a way of exploiting the structural regularity of Gray-coded high-order rectangular QAM, and transforms the classic symbol-based MIMO detection model to a low-complexity bit-based detection model. As an appealing benefit, the conventional three-step “signal-to-symbols-to-bits” decision process can be substituted by a simpler “signal-to-bits” decision process for the classic Gray-mapping aided high-order rectangular QAM, and hence any bit-based detection method becomes potentially applicable. As an application example, we propose a direct-bit-based VA-SDPR (DVA-SDPR) MIMO detector, which is capable of directly making binary decisions concerning the individual information bits of the ubiquitous Gray-mapping aided high-order rectangular QAM, while dispensing with symbol-based detection. Furthermore, the proposed model transformation method facilitates the exploitation of the unequal error protection (UEP) property of high-order QAM with the aid of the low-complexity bit-flipping based “hill climbing” method. As a result, the proposed DVA-SDPR detector achieves the best bit error ratio (BER) performance among the known SDPR-based MIMO detectors in the context considered, while still maintaining the lowest-possible worst-case complexity order of $O[(N_T \log_2 M + 1)^{3.5}]$.

Index Terms—Binary constrained quadratic programming, Gray mapping, primal-dual interior-point algorithm (PD-IPA),

Copyright (c) 2012 IEEE. Personal use of this material is permitted. However, permission to use this material for any other purposes must be obtained from the IEEE by sending a request to pubs-permissions@ieee.org.

The financial support of the China Scholarship Council (CSC), the EPSRC, UK under the auspices of the China-UK Science Bridges and that of the RC-UK under the India-UK Advanced Technology Centre (IU-ATC) is gratefully acknowledged. L. Hanzo would also like to acknowledge the fiscal support of the European Research Council’s Advanced Fellow Award.

This work was presented in part at the 2011 54th IEEE Global Communications Conference, Houston, Texas, USA (GLOBECOM 2011).

S. Yang is with the School of Electronics and Computer Science, University of Southampton, Southampton, SO17 1BJ, UK. He is also with the School of Information and Communication Engineering, Beijing University of Posts and Telecommunications, Beijing, 100876, China (email: sy7g09@ecs.soton.ac.uk).

Tiejun Lv is with the School of Information and Communication Engineering, Beijing University of Posts and Telecommunications, Beijing, 100876, China (email: lvtiejun@bupt.edu.cn).

L. Hanzo is with the School of Electronics and Computer Science, University of Southampton, Southampton, SO17 1BJ, UK (email: lh@ecs.soton.ac.uk).

high-order QAM, semidefinite programming relaxation (SDPR), virtually-antipodal detection.

I. INTRODUCTION

THE maximum-likelihood (ML) detection of rectangular quadrature amplitude modulation (QAM) in multiple-input-multiple-output (MIMO) systems constitutes an instance of the integer least-squares problem in vector space, which is known to be non-deterministic polynomial-time hard (NP-hard). The ML detection is optimal in the sense that it achieves the minimum symbol error probability under the assumption of equally probable input symbols. However, it imposes an exponentially increasing complexity which is on the order of $O(M^{N_T})$, where M is the constellation size and N_T is the number of transmit antennas. The tree-search based sphere decoder (SD) [1]–[3] represents probably the best-known class of computationally efficient algorithms capable of achieving the exact ML performance. However, the SD is only efficient for relatively high signal-to-noise ratios (SNRs) and small values of N_T , because it has an exponentially increasing *expected complexity order* of $O(M^{\beta N_T})$ in both the worst-case and the average-case, where $\beta \in (0, 1]$ is a small factor depending on the value of SNR [4]. Notably, a fixed-complexity sphere decoder (FCSD) was proposed for MIMO systems in [5]. It was shown that the FCSD achieves a near-ML performance with a complexity of $O(M^{\sqrt{N_T}})$ [6] regardless of the specific SNR encountered, which represents an attractive solution of facilitating an efficient hardware implementation compared to the exponential-complexity conventional SD.

In contrast to the classic tree-search philosophy, the semidefinite programming [7]–[9] relaxation (SDPR) approach is based on convex optimization theory [10] and has recently received much research attention [11]–[23]. The most attractive characteristic of the SDPR-aided detectors is that they guarantee a so-called polynomial-time¹ worst-case computational complexity, while achieving a high performance.

Most of the existing SDPR detectors are dependent on the specific modulation constellation. To elaborate a little further, SDPR was first proposed for a binary phase-shift keying (BPSK) modulated code-division multiple-access (CDMA) system [11], [12], and then it was extended to quadrature phase-shift keying (QPSK) [13]. Simulation results showed that the SDPR detector is capable of achieving a near-ML

¹The computational complexity increases as a polynomial function of N_T .

bit error ratio (BER) performance, when using BPSK [11] and QPSK [13]. The numerical and analytical results of [14], [15] confirmed that the SDPR detector achieves the maximum possible diversity order, when using BPSK for transmission over a real-valued fading MIMO channel. The SDPR approach was also further developed for high-order modulation schemes, such as for M -ary phase-shift keying (M -PSK) scenario in [16], [17], and for high-order rectangular QAM in [18]–[22]. As for the high-order QAM scenario, it was recently shown in [23] that the so-called polynomial-inspired SDPR (PI-SDPR) [18], the bound-constrained SDPR (BC-SDPR) [20] and the virtually antipodal SDPR (VA-SDPR) [22] are actually equivalent in the sense that they obtain the same symbol decisions, and hence exhibit an identical symbol error ratio (SER) performance². It should be noted however that for high-order modulation scenarios, the performance of the SDPR detectors is not so promising compared to that of the BPSK/QPSK scenario. Therefore, there is a need to further improve the performance of the SDPR based MIMO detector for high-order QAM constellations, while maintaining its low computational complexity.

The VA-SDPR detector is of particular interest to us, since it may be shown to have a strong connection to the SDPR detector used in BPSK, where the SDPR shows near-optimal performance. The VA-SDPR converts the non-binary integer programming problem into a binary integer programming problem. However, in the VA-SDPR detector of [22] the binary decisions are made on the “index bits” rather than on the “information bits”. These two types of bits are in general different from each other [22], except for the linear natural-mapping³ aided rectangular QAM [24]. More specifically, the Gray-mapping of rectangular M -QAM is nonlinear for $M > 4$. Therefore, as shown in [24], in contrast to the scenario of linear natural-mapping aided rectangular QAM, for Gray-mapping the relationship between the transmitted symbol vector \mathbf{s} and the associated antipodal information bit vector \mathbf{b} *cannot* be characterized by a compact linear matrix transformation of the form $\mathbf{s} = \mathbf{W}\mathbf{b}$, where \mathbf{W} is the constellation-specific modulation matrix known to both the transmitter and receiver. Consequently, when the ubiquitous Gray-mapping aided high-order rectangular QAM is used, in order to make correct decisions of the information bits, the VA-SDPR detector of [22] still has to obtain its symbol decisions first relying on the decided “index bits”.

Against this background, the major contributions of this

²More specifically, the solution equivalence between PI-SDR and BC-SDR holds for 16-QAM and 64-QAM, and that between BC-SDR and VA-SDR holds for any 4^q -QAM, where q is a positive integer. The SDPR QAM detector of [21] exhibits a better performance than that of [18], [20], [22], but has a much higher complexity.

³The linear natural mapping is defined as the mapping which satisfies eq.(3) of [24].

paper are as follows⁴.

1) We propose a novel model transformation method for MIMO systems using Gray-coded high-order rectangular QAM, which allows us to reformulate the classic symbol-based MIMO detection model as a simpler bit-based detection model. Gray-mapping is known to be nonlinear, and hence has made direct bit manipulation difficult to many detection methods. Our method is established by exploiting the structural regularity of Gray-coded high-order rectangular QAM with the aid of a strikingly simple linear matrix representation (LMR) of 4-QAM. As an appealing benefit, the conventional three-step “signal-to-symbols-to-bits” decision process can be replaced by a simpler “signal-to-bits” decision process for the classic Gray-mapping aided high-order rectangular QAM, and hence any bit-based detection method becomes potentially applicable.

2) Based on the above model transformation method, we propose a new direct-bit-based VA-SDPR (DVA-SDPR) detector for the ubiquitous Gray-mapping aided high-order rectangular QAM, which is capable of directly deciding on the information bits for transmission over fading MIMO channels. To elaborate a little further, our approach firstly transforms the original Gray-coded M -QAM aided $(N_T \times N_R)$ -element MIMO system to a virtual 4-QAM aided $(2N_T \times N_R)$ -element MIMO system. Since the modulation matrix of 4-QAM is identical for both the natural-mapping and the Gray-mapping [24], the proposed DVA-SDPR detector finally converts the classic nonlinear Gray-mapping aided M -QAM symbol detection problem to a Boolean quadratic programming (BQP) problem [10]. When relying on this technique, we can directly carry out the information-bit decisions without first invoking conventional symbol decisions for the nonlinear Gray-mapping aided rectangular M -QAM scheme.

3) Finally, the proposed model transformation method facilitates the exploitation of the unequal error protection (UEP) property of high-order QAM with the aid of the low-complexity bit-flipping based “hill climbing” method. As a beneficial result, the proposed DVA-SDPR detector achieves the best BER performance among the known SDPR-based MIMO detectors in the context considered, while still maintaining the lowest-possible polynomial-time worst-case complexity order of $O[(N_T \log_2 M + 1)^{3.5}]$.

The remainder of the paper is organized as follows. In Section II, our system model and the problem considered are presented. In Section III, the structure of Gray-coded high-order rectangular QAM constellations is scrutinized by considering both Gray-coded 16-QAM and 64-QAM as examples. As a result, the inherent relationship between the information bits of a QAM symbol is unveiled. Then, in Section IV the proposed DVA-SDPR detector is detailed from various

⁴Some initial results of this paper were briefly reported in [25], where only Gray-coded 16-QAM was considered. By contrast, in this paper we generalize the results of [25] to the M -QAM scenario, and detail the modified primal-dual interior point algorithm employed for solving the SDP problem considered. Additionally, the performance versus complexity tradeoff of the modified primal-dual interior-point algorithm with respect to its convergence accuracy is investigated, and the advantage of the proposed SDPR-based MIMO detector over the SD in the context of the emerging “massive” MIMO systems [26], [27] is elaborated on.

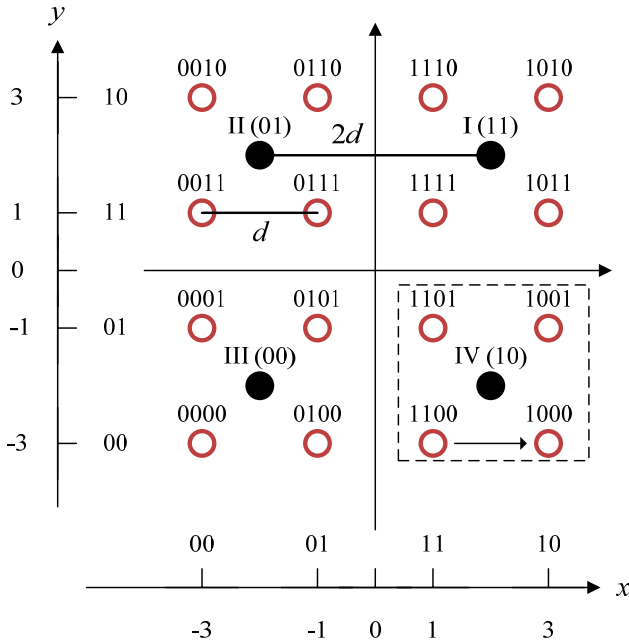


Fig. 1. Signal space diagram of the Gray-mapping aided 16-QAM.

perspectives, while our numerical results and discussions are presented in Section V. Finally, our conclusions are offered in Section VI.

Notation: Boldface uppercase letters and lowercase letters, as well as standard lowercase letters denote matrices, column vectors and scalars, respectively, while $(\cdot)^T$, $(\cdot)^H$ and $(\cdot)^{-1}$ denote the matrix transpose, conjugate transpose and matrix inverse, respectively. Furthermore, $\text{abs}(\cdot)$ represents the element-wise absolute value function, $\text{diag}(\mathbf{X})$ denotes the vector composed by the diagonal elements of matrix \mathbf{X} , and $\text{Diag}(\mathbf{v})$ represents a diagonal matrix with its diagonal elements being the vector \mathbf{v} . Additionally, \mathbb{Z}^+ denotes the set of all positive integers, \oplus is the XOR operator of two binary scalars, \boxplus represents the element-wise XOR operator of two binary vectors/matrices, and \otimes is the element-wise multiplication operation, while $\|\cdot\|_2$ represents the Euclidean norm. Finally, $\mathbf{X} \succeq 0$ and $\mathbf{X} \succ 0$ indicate that \mathbf{X} is a positive semidefinite (PSD) matrix and a positive definite matrix, respectively.

II. SYSTEM MODEL AND PROBLEM STATEMENT

Consider a symbol-synchronized memoryless spatial multiplexing MIMO system having N_T transmit and N_R receive antennas. The baseband equivalent system model is written as

$$\mathbf{y} = \mathbf{H}\mathbf{s} + \mathbf{n}, \quad (1)$$

where \mathbf{y} is the N_R -element received signal vector, \mathbf{s} is the N_T -element transmitted symbol vector, whose elements are from the Gray-coded rectangular M -QAM constellation, \mathbf{H} is the $(N_R \times N_T)$ -element complex-valued channel matrix, and \mathbf{n} is the N_R -element complex Gaussian noise vector with a zero mean and covariance matrix of $2\sigma^2\mathbf{I}$.

The ML detection conceived for the MIMO system of (1) can be formulated as the following constrained discrete least-squares optimization problem

$$\hat{\mathbf{s}}_{\text{ML}} = \arg \min_{\mathbf{s} \in \mathbb{D}} \|\mathbf{y} - \mathbf{H}\mathbf{s}\|_2^2, \quad (2)$$

where the alphabet set \mathbb{D} represents the Gray-mapping aided rectangular M -QAM constellation.

In [22], (2) was further formulated as⁵

$$\hat{\mathbf{d}}_{\text{ML}} = \arg \min_{\mathbf{d} \in \{+1, -1\}^{M_c N_T}} \|\tilde{\mathbf{y}} - \tilde{\mathbf{H}}\mathbf{T}\mathbf{d}\|_2^2, \quad (3)$$

where $M_c = \log_2 M$ denotes the number of bits per symbol, and \mathbf{d} represents the vector of “index bits” [22]⁶, which are different from the (antipodal) information-bit vector \mathbf{b} [22]. $\tilde{\mathbf{H}}$ and $\tilde{\mathbf{y}}$ are the real-valued versions of \mathbf{H} and \mathbf{y} in (2) respectively, while \mathbf{T} is the real-valued transformation matrix, which is fixed for a specific constellation, similar to the complex-valued modulation matrix \mathbf{W} of [24]. After obtaining $\hat{\mathbf{d}}_{\text{ML}}$, the original real-valued symbol vector corresponding to the real-valued system model is estimated as

$$\hat{\mathbf{s}}_{\text{ML}} = \mathbf{T}\hat{\mathbf{d}}_{\text{ML}}. \quad (4)$$

In contrast to this solution, the problem of interest to us is — how can we develop a VA-SDPR detector that directly estimates the (antipodal) information bit vector \mathbf{b} without estimating the symbol vector \mathbf{s} ?

III. REVISITING GRAY-MAPPING AIDED M -QAM

Assume that the j th component of the transmitted M -QAM symbol vector \mathbf{s} is obtained using the bit-to-symbol mapping function $s_j = \text{map}(\mathbf{u}_j)$, $j = 1, 2, \dots, N_T$, where $\mathbf{u}_j = [u_{j,1}, u_{j,2}, \dots, u_{j,M_c}]^T$ is the vector of information bits with each element being 1 or 0. The vector of information bits corresponding to \mathbf{s} is denoted as \mathbf{u} , which satisfies $\mathbf{s} = \text{map}(\mathbf{u})$ and is formed by concatenating the N_T antennas’ information bits $\mathbf{u}_1, \mathbf{u}_2, \dots, \mathbf{u}_{N_T}$, yielding $\mathbf{u} = [u_1, u_2, \dots, u_k, \dots, u_{M_c N_T}]^T = [\mathbf{u}_1^T, \mathbf{u}_2^T, \dots, \mathbf{u}_{N_T}^T]^T \in \{1, 0\}^{M_c N_T}$. The antipodal information bits are obtained from the original information bits of logical 1 or 0 using $b_k = 2u_k - 1$, where $b_k \in \{+1, -1\}$.

As shown in [24], the nonlinear Gray-mapping aided M -QAM scheme may be formulated as $\mathbf{s} = \mathbf{W}(\mathbf{b})\mathbf{b}$, where the structure of the modulation matrix $\mathbf{W}(\mathbf{b})$ exhibits multiple forms, depending on the antipodal information bit vector \mathbf{b} . Hence $\mathbf{W}(\mathbf{b})$ is not readily available at the receiver side. Although it may be possible to estimate the modulation matrix $\mathbf{W}(\mathbf{b})$ at the receiver, the estimation error will inevitably degrade the achievable performance.

As an instance, let us revisit the “generating units” of the Gray-mapping aided 16-QAM scheme shown in Table I [24]. Since the four constellation points in the same quadrant share the same generating units, without loss of generality, we will

⁵The real-valued model is used in [22], whereas we use the more general complex-valued model here.

⁶In general, the (real-valued) Gray-coded QAM symbol vector $\tilde{\mathbf{s}}$ cannot be represented as a linear transformation of $\tilde{\mathbf{s}} = \mathbf{T}\mathbf{b}$, as shown in [24]. However, it was formulated as $\tilde{\mathbf{s}} = \mathbf{T}\mathbf{d}$ in [22], where \mathbf{d} was termed as “index bits”.

TABLE I
GENERATING UNITS OF 16QAM USING GRAY MAPPING

Index	Generating Unit	Bit Sequence	Symbol	Quadrant	Index	Generating Unit	Bit Sequence	Symbol	Quadrant
1	$2 \ 1 \ 2i \ i$	$-1 \ -1 \ -1 \ -1$	$-3 \ -3i$	III	9	$2 \ -1 \ 2i \ i$	$+1 \ +1 \ -1 \ -1$	$1 \ -3i$	IV
2	$2 \ 1 \ 2i \ i$	$-1 \ -1 \ -1 \ +1$	$-3 \ -i$		10	$2 \ -1 \ 2i \ i$	$+1 \ +1 \ -1 \ +1$	$1 \ -i$	
3	$2 \ 1 \ 2i \ -i$	$-1 \ -1 \ +1 \ +1$	$-3 \ +i$	II	11	$2 \ -1 \ 2i \ -i$	$+1 \ +1 \ +1 \ +1$	$1 \ +i$	I
4	$2 \ 1 \ 2i \ -i$	$-1 \ -1 \ +1 \ -1$	$-3 \ +3i$		12	$2 \ -1 \ 2i \ -i$	$+1 \ +1 \ +1 \ -1$	$1 \ +3i$	
5	$2 \ 1 \ 2i \ -i$	$-1 \ +1 \ +1 \ -1$	$-1 \ +3i$		13	$2 \ -1 \ 2i \ -i$	$+1 \ -1 \ +1 \ -1$	$3 \ +3i$	
6	$2 \ 1 \ 2i \ -i$	$-1 \ +1 \ +1 \ +1$	$-1 \ +i$		14	$2 \ -1 \ 2i \ -i$	$+1 \ -1 \ +1 \ +1$	$3 \ +i$	
7	$2 \ 1 \ 2i \ i$	$-1 \ +1 \ -1 \ +1$	$-1 \ -i$	III	15	$2 \ -1 \ 2i \ i$	$+1 \ -1 \ -1 \ +1$	$3 \ -i$	IV
8	$2 \ 1 \ 2i \ i$	$-1 \ +1 \ -1 \ -1$	$-1 \ -3i$		16	$2 \ -1 \ 2i \ i$	$+1 \ -1 \ -1 \ -1$	$3 \ -3i$	

consider the constellation points in Quadrant IV of Fig. 1 as an example.

The legitimate original information-bit sequences $[u_1 \ u_2 \ u_3 \ u_4]$ are:

$$[1 \ \underline{1} \ 0 \ 0] \quad [1 \ 0 \ 0 \ 0] \quad [1 \ 0 \ 0 \ \underline{1}] \quad [1 \ \underline{1} \ 0 \ \underline{1}]. \quad (5)$$

The above-mentioned generating units $[g_1 \ g_2 \ g_3 \ g_4]$ corresponding to $[u_1 \ u_2 \ u_3 \ u_4]$ are:

$$[2 \ \underline{-1} \ 2i \ i] \quad [2 \ \underline{-1} \ 2i \ i] \quad [2 \ \underline{-1} \ 2i \ i] \quad [2 \ \underline{-1} \ 2i \ i]. \quad (6)$$

Observing (5) and (6), two remarks can be made. Firstly, the bits u_1 and u_3 of the four information-bit sequences that are mapped to the specific constellation points dwelling in the same quadrant are identical. Secondly, the first and the third components of the generating units are $[g_1 \ g_3] = [2 \ 2i]$, which indicates that the bits u_1 and u_3 of each information-bit sequence are mapped to a 4-QAM constellation, whose

amplitude is doubled⁷. Therefore, the Gray-mapping aided 16-QAM symbols of Quadrant IV can be formulated as

$$\begin{aligned} s &= \text{map}_{16\text{-QAM}}(u_1 \ u_2 \ u_3 \ u_4) \\ &= 2 \times \text{map}_{4\text{-QAM}}(u_1 \ u_3) + \text{map}_x(u_2 \ u_4) \\ &= 2s^{(1)} + s^{(2)}. \end{aligned} \quad (7)$$

To elucidate the notation of $\text{map}_x(u_2 \ u_4)$ further, let us observe

$$[u_2 \ u_4] : \quad [1 \ 0] \quad [0 \ 0] \quad [0 \ 1] \quad [1 \ 1], \quad (8)$$

$$[g_2 \ g_4] : \quad [-1 \ i] \quad [-1 \ i] \quad [-1 \ i] \quad [-1 \ i], \quad (9)$$

$$s^{(2)} : \quad -1-i \quad 1-i \quad 1+i \quad -1+i, \quad (10)$$

where we have $s^{(2)} = (2[u_2 \ u_4] - 1) \times [g_2 \ g_4]^T$. Note that

⁷As shown in [24], the natural-mapping and the Gray-mapping are identical for 4-QAM.

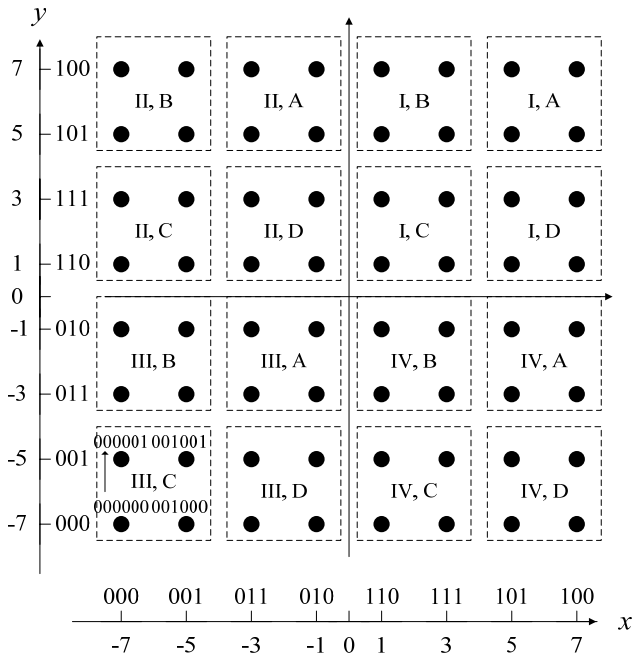


Fig. 2. Signal space diagram of the Gray-mapping aided 64-QAM.

$s^{(2)}$ may also be obtained by mapping the bits

$$[\tilde{u}_2 \ \tilde{u}_4] : \quad [0 \ 0] \quad [1 \ 0] \quad [1 \ 1] \quad [0 \ 1] \quad (11)$$

to 4-QAM, where $s^{(2)} = (2[\tilde{u}_2 \ \tilde{u}_4] - 1) \times [1 \ i]^T$.

Therefore, (7) may be reformulated as

$$s = 2 \times \text{map}_{4\text{-QAM}}(u_1 \ u_3) + \text{map}_{4\text{-QAM}}(\tilde{u}_2 \ \tilde{u}_4). \quad (12)$$

On the other hand, we notice that $[\tilde{u}_2 \ \tilde{u}_4]$ may be given by

$$\begin{aligned} 00 &= (\underline{1} \oplus 1)(\underline{0} \oplus 0), \\ 10 &= (\underline{0} \oplus 1)(\underline{0} \oplus 0), \\ 11 &= (\underline{0} \oplus 1)(\underline{1} \oplus 0), \\ 01 &= (\underline{1} \oplus 1)(\underline{1} \oplus 0), \end{aligned} \quad (13)$$

where \oplus represents the XOR operation. Eq. (13) may be rewritten in a more compact manner as

$$[\tilde{u}_2 \ \tilde{u}_4] = (u_2 \oplus u_1)(u_4 \oplus u_3) = [u_2 \ u_4] \boxplus [u_1 \ u_3], \quad (14)$$

hence we have

$$[u_2 \ u_4] = [u_1 \ u_3] \boxplus [\tilde{u}_2 \ \tilde{u}_4], \quad (15)$$

where \boxplus is the element-wise XOR operator. It may be readily shown that (14) and (15) also hold for the other three quadrants.

Similarly, the Gray-mapping aided 64-QAM symbols shown in Fig. 2 may be derived as

$$\begin{aligned} s &= \text{map}_{64\text{-QAM}}(u_1 \ u_2 \ u_3 \ u_4 \ u_5 \ u_6) \\ &= 2 \times \text{map}_{16\text{-QAM}}(u_1 \ u_2 \ u_4 \ u_5) + \text{map}_{4\text{-QAM}}(\tilde{u}_3 \ \tilde{u}_6) \\ &= 4 \times \text{map}_{4\text{-QAM}}(u_1 \ u_4) + 2 \times \text{map}_{4\text{-QAM}}(\tilde{u}_2 \ \tilde{u}_5) \\ &\quad + \text{map}_{4\text{-QAM}}(\tilde{u}_3 \ \tilde{u}_6) \\ &= 4s^{(1)} + 2s^{(2)} + s^{(3)}. \end{aligned} \quad (16)$$

where

$$[\tilde{u}_2 \ \tilde{u}_5] = [u_1 \ u_4] \boxplus [u_2 \ u_5], \quad (17)$$

and

$$[\tilde{u}_3 \ \tilde{u}_6] = (u_1 \oplus u_2 \oplus u_3)(u_4 \oplus u_5 \oplus u_6). \quad (18)$$

Hence we have

$$[u_2 \ u_5] = [u_1 \ u_4] \boxplus [\tilde{u}_2 \ \tilde{u}_5], \quad (19)$$

and

$$[u_3 \ u_6] = (u_1 \oplus u_2 \oplus \tilde{u}_3)(u_4 \oplus u_5 \oplus \tilde{u}_6). \quad (20)$$

The above transformation method can be extended to even higher-order rectangular QAM constellations. For clarity, we summarize their transformation formulae in Table II.

IV. THE PROPOSED DVA-SDPR DETECTOR

A. DVA-SDPR Formulation

For the sake of simplicity, below we will consider 16-QAM as an example to formulate the proposed DVA-SDPR detector.

Based on (12), the system model (1) can be rewritten as

$$\begin{aligned} \mathbf{y} &= [\mathbf{h}_1, \mathbf{h}_2, \dots, \mathbf{h}_{N_T}] \begin{bmatrix} 2s_1^{(1)} + s_1^{(2)} \\ 2s_2^{(1)} + s_2^{(2)} \\ \vdots \\ 2s_{N_T}^{(1)} + s_{N_T}^{(2)} \end{bmatrix} + \mathbf{n} \\ &= [2\mathbf{H} \ \mathbf{H}]\mathbf{x} + \mathbf{n}, \end{aligned} \quad (21)$$

where \mathbf{h}_j is the j th column of \mathbf{H} , $\mathbf{x} = [s_1^{(1)}, s_2^{(1)}, \dots, s_{N_T}^{(1)}, s_1^{(2)}, s_2^{(2)}, \dots, s_{N_T}^{(2)}]^T$ with each element being a standard 4-QAM symbol. At this stage, (21) may be regarded as a virtual 4-QAM aided $(2N_T \times N_R)$ -element MIMO system⁸.

According to the modulation matrix of 4-QAM given in [24], (21) can be further reformulated as

$$\mathbf{y} = [2\mathbf{H} \ \mathbf{H}]\mathbf{W}\mathbf{p} + \mathbf{n} = \mathbf{G}\mathbf{p} + \mathbf{n}, \quad (22)$$

where \mathbf{G} is the ‘‘composite channel matrix’’, $\mathbf{p} \in \{-1, +1\}^{M_c N_T}$, and

$$\mathbf{W} = \begin{bmatrix} 1 & i & 0 & 0 & \cdots & 0 & 0 \\ 0 & 0 & 1 & i & \cdots & 0 & 0 \\ 0 & 0 & 0 & 0 & \ddots & 0 & 0 \\ 0 & 0 & 0 & 0 & \cdots & 1 & i \end{bmatrix}_{\frac{M_c N_T}{2} \times M_c N_T} \quad (23)$$

is the modulation matrix of 4-QAM for both natural-mapping and Gray-mapping. Hence the original Gray-coded 16-QAM $(N_T \times N_R)$ -element MIMO channel has been converted to a virtual $(M_c N_T \times N_R)$ -element MIMO channel relying on binary signaling, where we have $M_c = 4$.

Therefore, the original ML detection related constrained discrete least-squares optimization problem of (2) may be reformulated as

$$\hat{\mathbf{p}}_{\text{ML}} = \arg \min_{\mathbf{p} \in \{+1, -1\}^{M_c N_T}} \|\mathbf{y} - \mathbf{G}\mathbf{p}\|_2^2, \quad (24)$$

which is shown to be equivalent to the following BQP problem [10]

$$\begin{aligned} \max \quad & 2\mathbf{y}^H \mathbf{G}\mathbf{p} - \mathbf{p}^T \mathbf{G}^H \mathbf{G}\mathbf{p} \\ \text{s. t.} \quad & \mathbf{p} \in \{+1, -1\}^{M_c N_T}, \end{aligned} \quad (25)$$

which is difficult to solve due to the non-convex constraints of $p_i^2 = 1$.

In order to cast the objective function of (25) into a homogeneous quadratic form, we introduce a redundant scalar $t \in \{+1, -1\}$. Since $t\mathbf{p} \in \{+1, -1\}^{M_c N_T}$ for any $\mathbf{p} \in \{+1, -1\}^{M_c N_T}$, (25) may also be formulated as

$$\begin{aligned} \max \quad & [\mathbf{p}^T \ t] \Re\{\mathbf{Q}_c\} [\mathbf{p}^T \ t]^T \\ \text{s. t.} \quad & [\mathbf{p}^T \ t] \in \{+1, -1\}^{M_c N_T + 1}, \end{aligned} \quad (26)$$

⁸This virtual MIMO system is not exactly equivalent to a real $(2N_T \times N_R)$ -element MIMO system, because the left half and the right half of the virtual channel matrix $[2\mathbf{H} \ \mathbf{H}]$ are fully correlated, both relying on \mathbf{H} .

TABLE II
GRAY-MAPPING BASED QAM TRANSFORMATION

16-QAM	$s = 2 \times \text{map}_{4\text{-QAM}}(u_1 u_3) + \text{map}_{4\text{-QAM}}(\tilde{u}_2 \tilde{u}_4)$, where $[\tilde{u}_2 \tilde{u}_4] = (u_1 \oplus u_2)(u_3 \oplus u_4)$
64-QAM	$s = 4 \times \text{map}_{4\text{-QAM}}(u_1 u_4) + 2 \times \text{map}_{4\text{-QAM}}(\tilde{u}_2 \tilde{u}_5) + \text{map}_{4\text{-QAM}}(\tilde{u}_3 \tilde{u}_6)$, where $[\tilde{u}_2 \tilde{u}_5] = (u_1 \oplus u_2)(u_4 \oplus u_5)$, $[\tilde{u}_3 \tilde{u}_6] = (u_1 \oplus u_2 \oplus u_3)(u_4 \oplus u_5 \oplus u_6)$
256-QAM	$s = 8 \times \text{map}_{4\text{-QAM}}(u_1 u_5) + 4 \times \text{map}_{4\text{-QAM}}(\tilde{u}_2 \tilde{u}_6) + 2 \times \text{map}_{4\text{-QAM}}(\tilde{u}_3 \tilde{u}_7) + \text{map}_{4\text{-QAM}}(\tilde{u}_4 \tilde{u}_8)$, where $[\tilde{u}_2 \tilde{u}_6] = (u_1 \oplus u_2)(u_5 \oplus u_6)$, $[\tilde{u}_3 \tilde{u}_7] = (u_1 \oplus u_2 \oplus u_3)(u_5 \oplus u_6 \oplus u_7)$, $[\tilde{u}_4 \tilde{u}_8] = (u_1 \oplus u_2 \oplus u_3 \oplus u_4)(u_5 \oplus u_6 \oplus u_7 \oplus u_8)$,
4^q -QAM	$s = 2^{q-1} \times \text{map}_{4\text{-QAM}}(u_1 u_{q+1}) + 2^{q-2} \times \text{map}_{4\text{-QAM}}(\tilde{u}_2 \tilde{u}_{q+2}) + \dots + 2 \times \text{map}_{4\text{-QAM}}(\tilde{u}_{q-1} \tilde{u}_{2q-1}) + \text{map}_{4\text{-QAM}}(\tilde{u}_q \tilde{u}_{2q})$, where $\tilde{u}_2 \tilde{u}_{q+2} = (u_1 \oplus u_2)(u_{q+1} \oplus u_{q+2})$, \vdots $[\tilde{u}_{q-1} \tilde{u}_{2q-1}] = (u_1 \oplus u_2 \oplus \dots \oplus u_{q-1})(u_{q+1} \oplus u_{q+2} \oplus \dots \oplus u_{2q-1})$ $[\tilde{u}_q \tilde{u}_{2q}] = (u_1 \oplus u_2 \oplus \dots \oplus u_q)(u_{q+1} \oplus u_{q+2} \oplus \dots \oplus u_{2q})$

where $\Re\{\mathbf{Q}_c\}$ represents the real part of the Hermitian matrix

$$\mathbf{Q}_c \triangleq \begin{bmatrix} -\mathbf{G}^H \mathbf{G} & \mathbf{G}^H \mathbf{y} \\ \mathbf{y}^H \mathbf{G} & 0 \end{bmatrix}. \quad (27)$$

Upon defining $\mathbf{x} \triangleq [\mathbf{p}^T t]^T$ and $\mathbf{Q} \triangleq \Re\{\mathbf{Q}_c\}$, (26) may be written in the following homogeneous quadratic form

$$\begin{aligned} \max \quad & \mathbf{x}^T \mathbf{Q} \mathbf{x} \\ \text{s. t.} \quad & \mathbf{x} \in \{+1, -1\}^{M_c N_T + 1}, \end{aligned} \quad (28)$$

where \mathbf{Q} is a symmetric matrix. Since we have $\mathbf{x}^T \mathbf{Q} \mathbf{x} = \text{Trace}(\mathbf{Q} \mathbf{x} \mathbf{x}^T) = \text{Trace}(\mathbf{x} \mathbf{x}^T \mathbf{Q})$, the problem of (28) may be equivalently rewritten as

$$\begin{aligned} \max \quad & \text{Trace}(\mathbf{X} \mathbf{Q}) \\ \text{s. t.} \quad & \mathbf{X} \succeq 0, \\ & \text{rank}(\mathbf{X}) = 1, \\ & \text{diag}(\mathbf{X}) = \mathbf{e}_{M_c N_T + 1}, \end{aligned} \quad (29)$$

where $\mathbf{X} = \mathbf{x} \mathbf{x}^T$, $\mathbf{x} \in \{+1, -1\}^{M_c N_T + 1}$, $\text{diag}(\mathbf{X})$ is the vector composed by the diagonal elements of \mathbf{X} , $\mathbf{e}_{M_c N_T + 1}$ is the ‘‘all-ones’’ vector of size $M_c N_T + 1$, and $\mathbf{X} \succeq 0$ indicates that \mathbf{X} is a symmetric and positive semidefinite (PSD) matrix. Due to the constraint of $\text{rank}(\mathbf{X}) = 1$, the problem (29) is non-convex, hence it is difficult to solve. However, by dropping the constraint of $\text{rank}(\mathbf{X}) = 1$, the problem of (29) may be relaxed to

$$\begin{aligned} \max \quad & \text{Trace}(\mathbf{X} \mathbf{Q}) \\ \text{s. t.} \quad & \mathbf{X} \succeq 0, \\ & \text{diag}(\mathbf{X}) = \mathbf{e}_{M_c N_T + 1}. \end{aligned} \quad (30)$$

The problem of (30) is known as an instance of semidefinite programming (SDP) [7], which constitutes a more general class of optimization techniques than linear programming⁹. Additionally, since SDP is a subclass of convex optimization,

⁹Several standard optimization problems, such as linear and quadratic programming can be unified under the framework of SDP [7].

it does not suffer from getting trapped in local minima¹⁰.

B. DVA-SDPR Solving Method

The SDP problem of (30) is solved using a modified version of the efficient primal-dual interior-point algorithm (PD-IPA) of [28] with arbitrarily high convergence accuracy, which guarantees a polynomial-time¹¹ worst-case complexity. The Lagrange dual problem associated with (30) is formulated as [11]

$$\begin{aligned} \min \quad & \mathbf{e}_{M_c N_T + 1}^T \mathbf{v} \\ \text{s. t.} \quad & \mathbf{Z} = \text{Diag}(\mathbf{v}) - \mathbf{Q} \succeq 0, \end{aligned} \quad (31)$$

where $\text{Diag}(\mathbf{v})$ represents a diagonal matrix with its diagonal elements being \mathbf{v} .

When the objective function values of the primal problem (30) and of its dual problem (31) satisfy

$$\mathbf{e}_{M_c N_T + 1}^T \mathbf{v} - \text{Trace}(\mathbf{X} \mathbf{Q}) \leq \max[1.0, \text{abs}(\mathbf{e}_{M_c N_T + 1}^T \mathbf{v})] \times \epsilon, \quad (32)$$

the PD-IPA is deemed to have converged, where the so-called convergence tolerance $\epsilon = 10^{-k}$ associated with an integer $k \geq 1$, controls the accuracy of convergence. The procedure of the modified version¹² of the PD-IPA is detailed as follows.

Input: the cost matrix \mathbf{Q} , the required convergence accuracy $\epsilon = 10^{-k}$, $k \in \mathbb{Z}^+$ and the singularity threshold $\tau = 10^{-n}$, $n \in \mathbb{Z}^+$.

Step 1: Initialization—Set the initial value of the number of iterations to $l = 0$; select a starting point $(\mathbf{X}_0, \mathbf{v}_0, \mathbf{Z}_0)$ so that it is in the interior of the feasible sets of both (30) and (31). For example, $\mathbf{X}_0 = \text{Diag}(\mathbf{e}_{M_c N_T + 1}) \succ 0$, $\mathbf{v}_0 = \text{abs}(\mathbf{Q}) \times \mathbf{e}_{M_c N_T + 1} \times 1.1$, $\mathbf{Z}_0 = \text{Diag}(\mathbf{v}_0) - \mathbf{Q} \succ 0$, where $\text{abs}(\cdot)$ represents the element-wise absolute value function.

¹⁰This does not mean that the SDPR detector is always capable of achieving the optimal ML performance, because the problem of (30) is a relaxed version of the original ML optimization problem of (25).

¹¹The complexity increases as a polynomial function of the problem size, which is determined by the number of rows (or columns) of the symmetric cost matrix \mathbf{Q} of (30) in the considered context. Here \mathbf{Q} is the input argument of the PD-IPA employed.

¹²For details of the modifications we have made regarding the original PD-IPA, please refer to the Remark following Step 2.4.

Set the initial value of the primal and dual costs to $C_0^p = \text{Trace}(\mathbf{X}_0 \mathbf{Q})$ and to $C_0^d = \mathbf{e}_{M_c N_T + 1}^T \mathbf{v}_0$, respectively.

Set the initial value of the penalty parameter to $\mu_0 = \frac{0.5 \times \text{Trace}(\mathbf{X}_0 \mathbf{Z}_0)}{M_c N_T + 1}$.

Set the initial value of the positive definiteness indicator of \mathbf{Z}_0 to $f_0^{pd} = 1$.

Step 2: Search loop—while both $(C_l^d - C_l^p > \max([1.0, \text{abs}(C_l^d)] \times \epsilon))$ and $(f_l^{pd} = 1)$ hold true:

Step 2.1: Compute $(\Delta \mathbf{X}, \Delta \mathbf{v}, \Delta \mathbf{Z})$, which determines the search direction using

$$\Delta \mathbf{v} = \left((\mathbf{Z}_l^{-1} \otimes \mathbf{X}_l)^{-1} \right) \times \mu_l \text{diag}(\mathbf{Z}_l^{-1}) - \mathbf{e}_{M_c N_T + 1}, \quad (33)$$

$$\Delta \mathbf{Z} = \text{Diag}(\Delta \mathbf{v}), \quad (34)$$

$$\Delta \hat{\mathbf{X}} = \mu_l \mathbf{Z}_l^{-1} - \mathbf{X}_l - \mathbf{Z}_l^{-1} \Delta \mathbf{Z} \mathbf{X}_l, \quad (35)$$

$$\Delta \mathbf{X} = 0.5 \times \left(\Delta \hat{\mathbf{X}} + \Delta \hat{\mathbf{X}}^T \right), \quad (36)$$

where \otimes represents the element-wise multiplication operation.

Step 2.2: Execute line search on the primal problem (resp. the dual problem), and update \mathbf{X}_l (resp. \mathbf{v}_l and \mathbf{Z}_l) and μ_l :

Set the initial step size to $\alpha_p = 1.0$ (resp. $\alpha_d = 1.0$), then invoke Cholesky decomposition to determine whether $\mathbf{X}_l + \alpha_p \Delta \mathbf{X}$ (resp. $\mathbf{Z}_l + \alpha_d \Delta \mathbf{Z}$) is positive-definite or not. If $\mathbf{X}_l + \alpha_p \Delta \mathbf{X} \succ 0$ (resp. $\mathbf{Z}_l + \alpha_d \Delta \mathbf{Z} \succ 0$), let $\mathbf{X}_{l+1} = \mathbf{X}_l + \alpha_p \Delta \mathbf{X}$ (resp. $\mathbf{v}_{l+1} = \mathbf{v}_l + \alpha_d \Delta \mathbf{v}$ and $\mathbf{Z}_{l+1} = \mathbf{Z}_l + \alpha_d \Delta \mathbf{Z}$).

Otherwise, reduce the step size to $\alpha'_p = \eta \alpha_p$ (resp. $\alpha'_d = \eta \alpha_d$), where $\eta \in (0, 1)$, e.g. $\eta = 0.8$, until $\mathbf{X}_l + \alpha'_p \Delta \mathbf{X} \succ 0$ (resp. $\mathbf{Z}_l + \alpha'_d \Delta \mathbf{Z} \succ 0$) holds; then set $\alpha''_p = \gamma \alpha'_p$ (resp. $\alpha''_d = \gamma \alpha'_d$), where $\eta < \gamma < 1.0$ holds true, e.g. $\gamma = 0.95$, so that the currently selected interim point is not on the boundary but in the interior of the corresponding feasible region, and let $\mathbf{X}_{l+1} = \mathbf{X}_l + \alpha''_p \Delta \mathbf{X}$ (resp. $\mathbf{v}_{l+1} = \mathbf{v}_l + \alpha''_d \Delta \mathbf{v}$ and $\mathbf{Z}_{l+1} = \mathbf{Z}_l + \alpha''_d \Delta \mathbf{Z}$).

Subsequently, update the penalty parameter using $\mu_{l+1} = \frac{0.5 \times \text{Trace}(\mathbf{X}_{l+1} \mathbf{Z}_{l+1})}{M_c N_T + 1}$, and if $\alpha''_p + \alpha''_d > 1.8$ (or initially, $\alpha_p + \alpha_d > 1.8$), the current value of μ_{l+1} should be further reduced to $0.5\mu_{l+1}$.

Step 2.3: Update the value of the primal and dual costs using $C_{l+1}^p = \text{Trace}(\mathbf{X}_{l+1} \mathbf{Q})$ and $C_{l+1}^d = \mathbf{e}_{M_c N_T + 1}^T \mathbf{v}_{l+1}$, respectively.

Step 2.4: Calculate the eigenvalues λ_i of the matrix \mathbf{Z}_{l+1} , $i = 1, 2, \dots, M_c N_T + 1$. If $\exists \text{abs}(\lambda_i) < \tau$, let the positive definiteness indicator of \mathbf{Z}_{l+1} be $f_{l+1}^{pd} = 0$, and terminate the search loop in advance. Otherwise, let $f_{l+1}^{pd} = 1$ and $l = l + 1$, and if the condition $(C_l^d - C_l^p > \max([1.0, \text{abs}(C_l^d)] \times \epsilon))$ holds true as well, repeat Step 2 until the stopping criteria of the search loop are satisfied, and return the solution matrix $\mathbf{X}^* = \mathbf{X}_l$ as the output.

Remark: Note that as μ_l approaches zero, \mathbf{Z}_l tends to be nearly singular, which potentially leads to a degraded numerical stability of the PD-IPA algorithm considered, because the computation of \mathbf{Z}_l^{-1} is explicitly involved. In order to circumvent this problem, the eigenvalues of \mathbf{Z}^{-1} are examined in Step 2.4 to ensure that the matrix \mathbf{Z}_l employed in the modified PD-IPA always remains positive-definite, and hence the accuracy of the output solution matrix \mathbf{X}^* is not affected. Additionally, the search loop can be curtailed whenever \mathbf{Z}_l is deemed to be singular, because the value of the positive definiteness indicator f_0^{pd} of \mathbf{Z}_l is introduced as another condition for allowing the search loop to proceed. As a result, the potentially unnecessary computations are avoided. ■

After obtaining the solution matrix \mathbf{X}^* of the problem (30), the solution vector \mathbf{p}^* of the problem (25) may be derived with the aid of several post-processing techniques [18], among which the simplest one is

$$\mathbf{p}^* = \text{sgn}(\mathbf{X}_{1:M_c N_T, M_c N_T + 1}), \quad (37)$$

with $\mathbf{X}_{1:M_c N_T, M_c N_T + 1}$ denoting the first $M_c N_T$ elements of the last column of \mathbf{X} . For 16-QAM, as shown by (12), the vector $\hat{\mathbf{u}} = (\mathbf{p}^* + \mathbf{e}_{M_c N_T})/2$ contains half of the original information bit vector \mathbf{u}^* . The remaining half of \mathbf{u}^* may be obtained from $\hat{\mathbf{u}}$ with the aid of the element-wise XOR operations of (15). On the other hand, for 64-QAM, (16) indicates that the vector $\hat{\mathbf{u}} = (\mathbf{p}^* + \mathbf{e}_{M_c N_T})/2$ contains two original information bits, namely u_1 and u_4 , and the remaining four information bits may be obtained from $\hat{\mathbf{u}}$ by using the element-wise XOR operations of (19) and (20).

C. Performance Refinement Using Bit-Flipping

The proposed DVA-SDPR detector exhibits the UEP property for the bits in different positions of a single M -QAM symbol¹³. This may be explained with the aid of, for example (12), where the bits u_1 and u_3 are mapped to a 4-QAM constellation having a doubled amplitude. Inspired by this observation, corresponding to (22), each time we may flip the sign of the i th bit p_i^* of \mathbf{p}^* , $i = \frac{M_c N_T}{2} + 1, \dots, M_c N_T$, to obtain a modified solution vector $\tilde{\mathbf{p}}_i^*$. There will be a total of $\frac{M_c N_T}{2}$ modified solution vectors. The final solution vector is chosen as the one, which minimizes $\|\mathbf{y} - \mathbf{G}\mathbf{p}\|_2^2$, when considering \mathbf{p}^* and $\tilde{\mathbf{p}}_i^*$. For 64-QAM, a similar bit-flipping technique may be used corresponding to (16).

D. Complexity Analysis

The SDP problem of (30) involves a matrix variable \mathbf{X} of size $(M_c N_T + 1) \times (M_c N_T + 1)$, which entails a computational complexity of $O\left[(M_c N_T + 1)^{3.5}\right]$, when employing the above-mentioned modified version of the PD-IPA of [28]. The complexity of the $\text{sgn}(\cdot)$ operations of (37), the XOR operations of for example (15), (19) and (20), the operations of the bit-flipping as well as the related Euclidean distance computations do not affect the complexity order. Hence the overall complexity of recovering the original information bit vector is on the order of $O\left[(M_c N_T + 1)^{3.5}\right]$.

V. SIMULATION RESULTS AND DISCUSSIONS

In this section, without loss of generality, we characterize the proposed DVA-SDPR MIMO detector's achievable performance versus the computational complexity in the scenario of the classic Gray-mapping aided 16-QAM using Monte Carlo (MC) simulations. The average SNR per receive antenna is defined as

$$\begin{aligned} \text{SNR} &\triangleq 10 \log_{10} \left(E \left\{ \|\mathbf{H}\mathbf{s}\|^2 / N_R \right\} / 2\sigma^2 \right) \\ &= 10 \log_{10} (N_T / 2\sigma^2). \end{aligned} \quad (38)$$

The computational complexity is quantified in terms of the number of equivalent additions, denoted as N_{add} , required for decoding a single transmitted MIMO symbol vector. More explicitly, we have $N_{\text{add}} \triangleq E\{T_{\text{tot}}\} / E\{T_{\text{add}}\}$, where T_{tot} is the average time required for decoding a MIMO symbol vector, while T_{add} is the average computation-time per addition

¹³Please refer to the description of Fig. 5 in Section V.

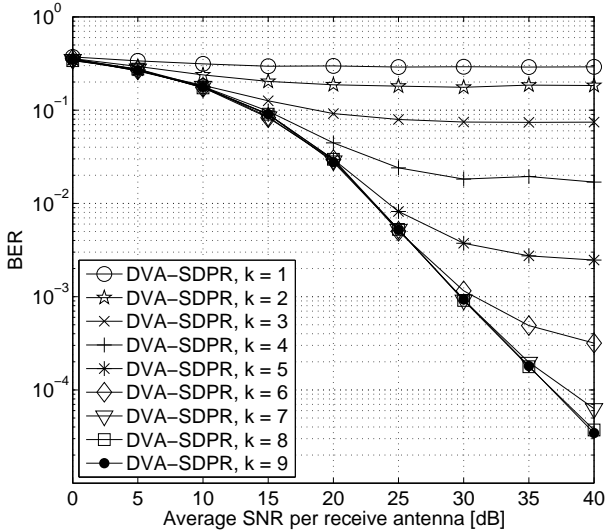


Fig. 3. Impact of the convergence tolerance $\epsilon = 10^{-k}$ on the performance of the DVA-SDPR for 16-QAM aided (8×8) -element MIMO over uncorrelated flat Rayleigh fading channels.

operation. Compared to the “execution-time” metric used in [20], this complexity metric has the advantage of being independent of different simulation platforms¹⁴. An (8×8) -element flat Rayleigh fading MIMO channel is considered, where the MIMO channel-matrix entries are chosen as independent and identically distributed (i.i.d.), zero mean, unit-variance complex-valued Gaussian random variables. Hence the system’s total throughput is $8 \times 4 = 32$ bits/MIMO symbol vector. A new realization of the channel matrix is drawn for each transmitted symbol vector. Each element of the noise vector \mathbf{n} is i.i.d. and $\mathcal{CN}(0, 2\sigma^2)$. Since it has been shown that the SDPR detectors of [18], [20] and [22] are equivalent in performance, below we will consider the IVA-SDPR of [22] as one of the benchmarks.

A. Simulation Results

Fig. 3 quantified the impact of the convergence tolerance ϵ on the performance of the DVA-SDPR MIMO detector. We can observe from Fig. 3 that for ϵ being represented by an 8-digit ($k = 8$) and 9-digit ($k = 9$) accuracy, the DVA-SDPR detector achieved an almost identical performance. By contrast, Fig. 4 represents the impact of the convergence tolerance ϵ on the computational complexity of the DVA-SDPR detector. It can be observed that the complexity of the DVA-SDPR detector increased almost uniformly upon increasing the number of digits. Based on these observations, we use $\epsilon = 10^{-9}$ in the following numerical experiments related to the DVA-SDPR detector.

Fig. 5 provided an insight into the UEP characteristics of the proposed DVA-SDPR detector. Observe in the figure that the first and the third bits (resp. the second and the fourth

¹⁴For a given algorithm, both T_{tot} and T_{add} should be measured in the same simulation platform, where T_{add} serves as a normalizing unit.

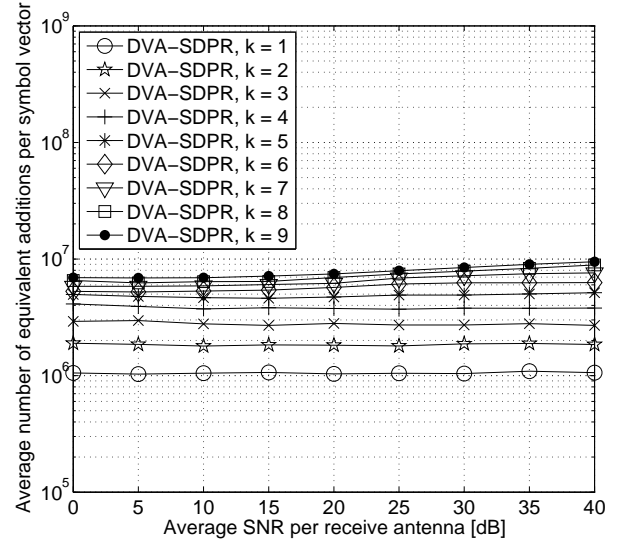


Fig. 4. Impact of the convergence tolerance $\epsilon = 10^{-k}$ on the complexity of the DVA-SDPR for 16-QAM aided (8×8) -element MIMO over uncorrelated flat Rayleigh fading channels.

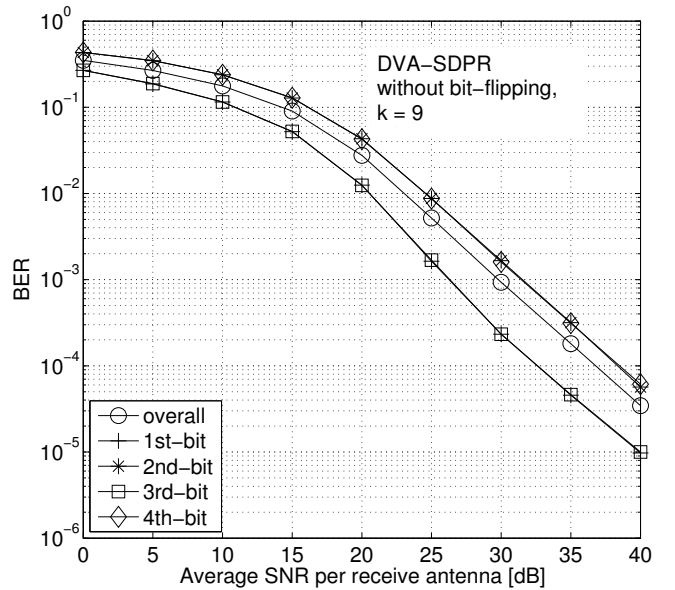


Fig. 5. Unequal error protection of the DVA-SDPR for Gray-coded 16-QAM aided (8×8) -element MIMO over uncorrelated flat Rayleigh fading channels, with the convergence tolerance $\epsilon = 10^{-9}$.

bits), namely u_1 and u_3 (resp. u_2 and u_4) of a single 16-QAM symbol exhibit an identical BER performance, which is better (resp. worse) than the overall BER performance.

In Fig. 6, we contrasted the BER performance of the proposed DVA-SDPR (with or without bit-flipping) to that of these benchmarks, namely to that of the IVA-SDPR of [22], of the minimum-mean-square-error-ordered-successive-interference-cancellation (MMSE-OSIC), and of the SD relying on an adaptive sphere radius for the sake of achieving

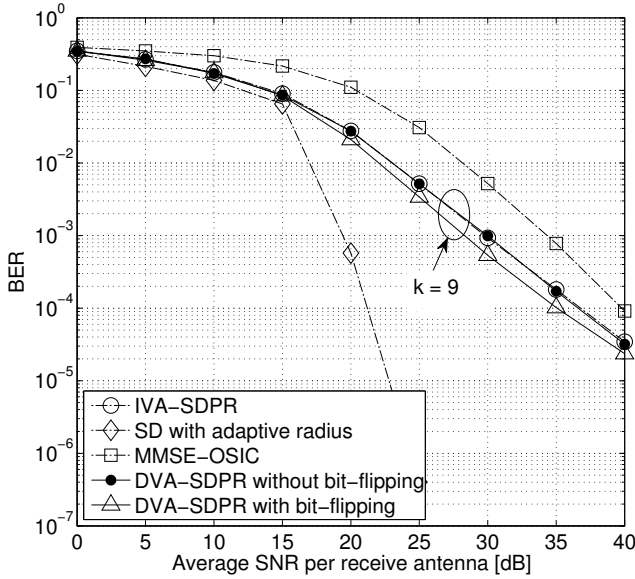


Fig. 6. Performance comparison of the DVA-SDPR, IVA-SDPR, SD and MMSE-OSIC detectors for 16-QAM aided (8×8) -element MIMO over uncorrelated flat Rayleigh fading channels.

the exact ML performance¹⁵. Observe in Fig. 6 that the proposed DVA-SDPR detector operating without bit-flipping achieves a BER performance identical to that of the IVA-SDPR benchmarker. By contrast, the bit-flipping aided DVA-SDPR outperforms the IVA-SDPR by about 2dB at BER = 10^{-3} and BER = 10^{-4} . As expected, all the SDPR detectors considered exhibit a superior BER performance compared to the MMSE-OSIC detector. However, unlike in the BPSK scenario, where the SDPR detector achieves the maximum attainable diversity [15], in the 16-QAM scenario considered, the DVA-SDPR and IVA-SDPR detectors suffer from a considerable performance degradation in the high SNR region compared to the SD. This indicates that the SDPR detectors considered might not be able to achieve full diversity for the Gray-coded 16-QAM aided (8×8) -element MIMO fading channel.

In Fig. 7, we compared the complexity of the detectors considered in Fig. 6. It is readily seen that the SD imposed a significantly higher computational complexity in the low-SNR region than in the high-SNR region, which is consistent with the theoretical results of [4]. By comparison, the computational complexities of both the proposed DVA-SDPR detectors operating with and without bit-flipping as well as the IVA-SDPR detector are near-constant. More specifically, the DVA-SDPR dispensing with bit-flipping has a slightly lower complexity than the IVA-SDPR benchmarker, since the IVA-SDPR detector requires the computation of Eq. (4) plus the computation of 16 Euclidean distances for deciding upon each transmitted 16-QAM symbol, before proceeding to the information-bit decisions. On the other hand, the DVA-SDPR using bit-flipping imposes a computational complexity near-identical to that of the IVA-SDPR. Furthermore, the complex-

¹⁵This SD is based on the classic SD of [1], and the minimum sphere radius was set to 2.

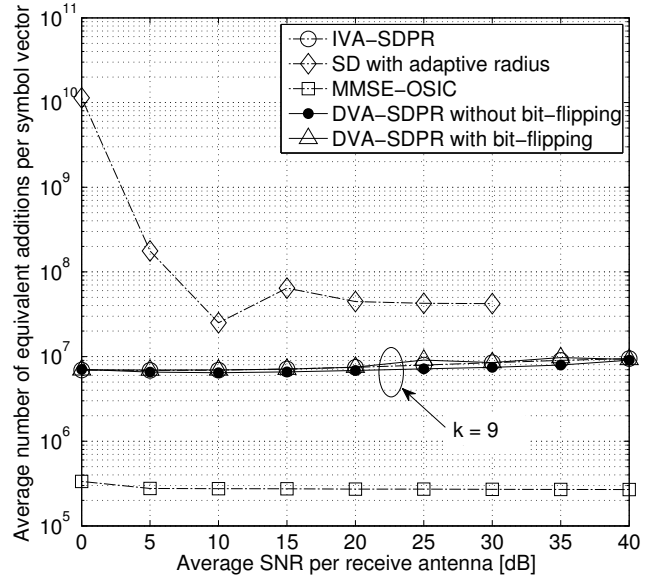


Fig. 7. Complexity comparison of the DVA-SDPR, IVA-SDPR, SD and MMSE-OSIC detectors for 16-QAM aided (8×8) -element MIMO.

ity of both the IVA-SDPR and the DVA-SDPR detectors is considerably lower than that of the SD detector. For example, the complexity of the SD at SNR = 0dB is over 1000 times higher than that of the DVA-SDPR, and is still about 7 times higher than that of the DVA-SDPR in the high-SNR region. Nonetheless, as expected, the complexity of the SDPR based detectors is still higher than that of the MMSE-OSIC detector.

Finally, in Fig. 8 we compared the complexity of the DVA-SDPR, the classic SD as well as the FCSD detectors in the context of “massive” MIMOs [26], [27], where the number of transmit antennas can be very high. Indeed, the employment of “massive” MIMOs becomes potentially important in the emerging heterogeneous wireless communication systems using the millimeter-wave band. This is because at millimetric wavelength hundreds of low-cost antenna-elements may be integrated into the backplane of laptops and mobile phones for the sake of compensating for the increased pathloss [27]. It is observed in Fig. 8 that the DVA-SDPR detector has a significantly lower computational complexity compared to the SD, especially when N_T is high. Additionally, the FCSD also shows a dramatically reduced complexity compared to the SD, but it still has a higher complexity than the DVA-SDPR detector, when N_T is very high. This implies that although the SD based detectors are competitive at the time of writing in the relatively low-throughput MIMO systems associated with moderate values of N_T , it might be difficult to use them in the “massive” MIMO systems of the near future [26], [27], where the DVA-SDPR detector might be more promising.

B. Discussions

1) To the best of our knowledge, in the uncoded Gray-mapping aided 16-QAM (8×8) -element MIMO scenario considered, the DVA-SDPR using bit-flipping achieves the

best BER performance result among the known SDPR-aided MIMO detectors, while still maintaining a polynomially increasing worst-case complexity order of $O[(M_c N_T + 1)^{3.5}]$. Additionally, since the proposed DVA-SDPR detector directly generates the information-bit decisions without first making symbol decisions, it may reduce the hardware cost in practical applications. In general, the DVA-SDPR, the IVA-SDPR and the MMSE-OSIC detectors may serve as efficient alternatives for the SD in the low-SNR region, say below about 15dB in the context considered. The SDPR detectors achieve full-diversity in a BPSK scenario, hence an interesting problem for future research is to conceive efficient SDPR detectors that can approach the ML performance for high-order QAM.

2) In practical MIMO systems, typically channel coding is applied and a powerful iterative detection and decoding based receiver is employed. In order to facilitate its application in coded systems, the SDP based MIMO detector has to output soft information. Indeed, there have been some efforts dedicated to extending the SDP based detection to the soft-input soft-output scenario. However, because most of the existing SDP based hard MIMO detectors are dependent on the specific modulation constellation, most of the available *soft* SDP detectors are only capable of estimating unknown binary variables. For example, the soft SDP-based MIMO detectors proposed in [29], [30] are only applicable to BPSK and QPSK (since a QPSK symbol can be treated equivalently to two BPSK symbols). As a further effort, the authors of [31] proposed a soft SDP based MIMO detector for 16-QAM, which is not applicable to other high-order QAM constellations. Since the virtually-antipodal SDP detector proposed in this paper transforms the symbol detection of the general rectangular M -QAM constellations to BPSK-like detection, the existing soft SDP detectors devised for estimating unknown binary vari-

ables are expected to be immediately applicable to facilitating the soft-detection in MIMO systems relying on high-order rectangular QAM. However, because the soft SDP detection is beyond the scope of this paper, it may be investigated in our future work.

3) Although the empirical results found in both the open literature and in this paper imply that the SDP based MIMO-QAM detectors experience a considerable performance loss, so far little has been known about the theoretical performance of the SDP based MIMO-QAM detector¹⁶. Indeed, the theoretical performance of the SDP based MIMO detector is relatively well-understood in the case of a BPSK scenario. More specifically, it was shown that the SDP based MIMO detector achieves the maximum possible receiver diversity order in the high-SNR region, as the ML detector does, when assuming a real-valued channel matrix [15].

Unfortunately, the performance analysis provided in [15] *cannot* be extended to the scenario of QAM constellations, because the analysis presented in [15] depends crucially on the structure of the channel matrix. More specifically, in the scenario of a channel matrix having real-valued elements corresponding to BPSK modulation, the rotational symmetry of the distribution of the channel matrix is explicitly exploited for proving that the SDP based MIMO detector is capable of achieving the maximum attainable diversity order. However, for the scenario of a channel matrix having complex-valued elements corresponding to QAM constellations, the rotational symmetry of the channel matrix is lost, even when the channel matrix is i.i.d. circularly symmetric zero-mean complex Gaussian [15]. It was shown in [15] that the SDP based MIMO

¹⁶There is only one paper investigating the SDP based MIMO detector's diversity-order performance to date, but it is limited to BPSK scenario, as seen in [15].

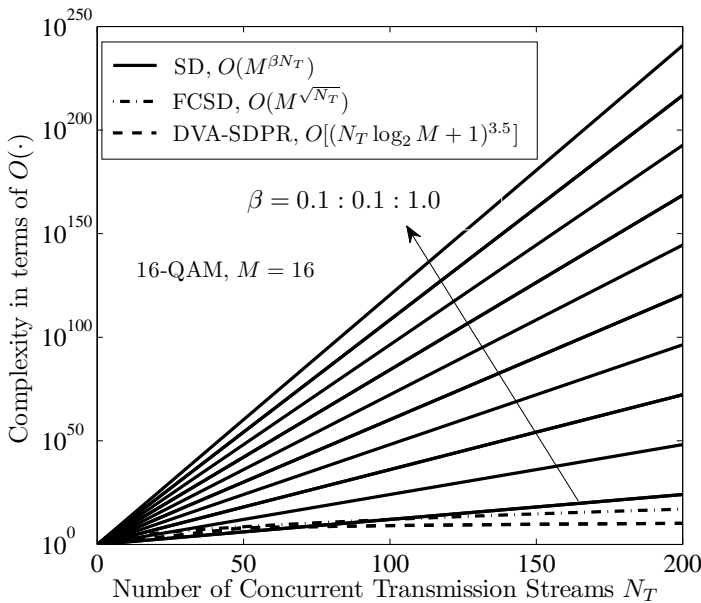


Fig. 8. Complexity comparison of the DVA-SDPR and the SD based detectors for 16-QAM aided massive MIMOs where the value of N_T can be very high.

detector appears to experience a modest loss in diversity gain even for 4-QAM, although the complex-valued channel matrix has been rewritten in an equivalent real-valued form.

In our paper, the SDP based MIMO-QAM detector is reformulated as a virtually BPSK-like MIMO detector, which facilitates the employment of bit-flipping for improving the SDP based MIMO-QAM detector's performance. Additionally, this transformation might be helpful for analyzing the SDP based MIMO-QAM detector's performance, because it has a close connection to the SDP based MIMO-BPSK detector. To elaborate a little further, due to the transformation presented in this paper, it has become possible to invoke the analytical results previously obtained for the SDP based MIMO-BPSK detector for the sake of assisting the performance analysis of the SDP based MIMO-QAM detectors. For instance, we can now infer that the structure of the "equivalent" channel matrix in our BPSK-like signal model is responsible for the diversity-order loss experienced by high-order QAM constellations. The more rigorous and comprehensive theoretical performance analysis of the SDP based MIMO-QAM detectors is an interesting problem to tackle in our future work.

VI. CONCLUSIONS

In contrast to the existing IVA-SDPR detector, the proposed DVA-SDPR detector bypasses symbol-decisions and directly generates the information bits of classic Gray-mapping aided M -QAM by employing a simple linear matrix representation of 4-QAM. Based on this contribution, the MIMO detector and constellation demapper modules of high-order rectangular QAM using either linear natural mapping or nonlinear Gray mapping may be replaced by a single DVA-SDPR detector, which performs detection and demapping jointly. Furthermore, when combined with low-complexity bit-flipping based "hill climbing" method, the proposed DVA-SDPR detector achieves the best BER performance among the known SDPR-based detectors in the context considered, while still maintaining the lowest-possible polynomial-time worst-case complexity order of $O[(N_T \log_2 M + 1)^{3.5}]$.

REFERENCES

- [1] E. Viterbo and J. Boutros, "A universal lattice code decoder for fading channels," *IEEE Transactions on Information Theory*, vol. 45, no. 7, pp. 1639–1642, Jul. 1999.
- [2] L. Hanzo, Y. Akhtman, L. Wang, and M. Jiang, *MIMO-OFDM for LTE, Wi-Fi and WiMAX: Coherent versus Non-Coherent and Cooperative Turbo-Transceivers*. Chichester, UK: Wiley, 2010.
- [3] Z. Y. Shao, S. W. Cheung, and T. I. Yuk, "Combined semi-definite relaxation and sphere decoding method for multiple antennas systems," in *Proc. International ITG Workshop on Smart Antennas (WSA'11)*, Feb. 2011, pp. 1–4.
- [4] J. Jaldén and B. Ottersten, "On the complexity of sphere decoding in digital communications," *IEEE Transactions on Signal Processing*, vol. 53, no. 4, pp. 1474–1484, Apr. 2005.
- [5] L. Barbero and J. Thompson, "Fixing the complexity of the sphere decoder for mimo detection," *IEEE Transactions on Wireless Communications*, vol. 7, no. 6, pp. 2131–2142, Jun. 2008.
- [6] J. Jaldén, L. Barbero, B. Ottersten, and J. Thompson, "The error probability of the fixed-complexity sphere decoder," *IEEE Transactions on Signal Processing*, vol. 57, no. 7, pp. 2711–2720, Jul. 2009.
- [7] L. Vandenberghe and S. Boyd, "Semidefinite programming," *SIAM Review*, vol. 38, no. 1, pp. 49–95, Mar. 1996.
- [8] Z.-Q. Luo, W.-K. Ma, A. So, Y. Ye, and S. Zhang, "Semidefinite relaxation of quadratic optimization problems," *IEEE Signal Processing Magazine*, vol. 27, no. 3, pp. 20–34, May 2010.
- [9] Z.-Q. Luo and W. Yu, "An introduction to convex optimization for communications and signal processing," *IEEE Journal on Selected Areas in Communications*, vol. 24, no. 8, pp. 1426–1438, Aug. 2006.
- [10] S. Boyd and L. Vandenberghe, *Convex Optimization*. New York, USA: Cambridge University Press, 2004.
- [11] P. H. Tan and L. K. Rasmussen, "The application of semidefinite programming for detection in CDMA," *IEEE Journal on Selected Areas in Communications*, vol. 19, no. 8, pp. 1442–1449, Aug. 2001.
- [12] W.-K. Ma, T. N. Davidson, K. M. Wong, Z.-Q. Luo, and P.-C. Ching, "Quasi-maximum-likelihood multiuser detection using semi-definite relaxation with application to synchronous CDMA," *IEEE Transactions on Signal Processing*, vol. 50, no. 4, pp. 912–922, Apr. 2002.
- [13] W.-K. Ma, T. N. Davidson, K. M. Wong, and P.-C. Ching, "A block alternating likelihood maximization approach to multiuser detection," *IEEE Transactions on Signal Processing*, vol. 52, no. 9, pp. 2600–2611, Sep. 2004.
- [14] M. Kisialiou and Z.-Q. Luo, "Performance analysis of quasi-maximum-likelihood detector based on semi-definite programming," in *Proc. IEEE International Conference on Acoustics, Speech, and Signal Processing (ICASSP'05)*, vol. 3, Philadelphia, PA, Mar. 2005, pp. III/433–III/436.
- [15] J. Jaldén and B. Ottersten, "The diversity order of the semidefinite relaxation detector," *IEEE Transactions on Information Theory*, vol. 54, no. 4, pp. 1406–1422, Apr. 2008.
- [16] Z.-Q. Luo, X. Luo, and M. Kisialiou, "An efficient quasi-maximum likelihood decoder for PSK signals," in *Proc. IEEE International Conference on Acoustics, Speech, and Signal Processing (ICASSP'03)*, vol. 6, Hong Kong, China, Apr. 2003, pp. VI/561–VI/564.
- [17] W.-K. Ma, P.-C. Ching, and Z. Ding, "Semidefinite relaxation based multiuser detection for M-ary PSK multiuser systems," *IEEE Transactions on Signal Processing*, vol. 52, no. 10, pp. 2862–2872, Oct. 2004.
- [18] A. Wiesel, Y. C. Eldar, and S. S. Shitz, "Semidefinite relaxation for detection of 16-QAM signaling in MIMO channels," *IEEE Signal Processing Letters*, vol. 12, no. 9, pp. 653–656, Sep. 2005.
- [19] Y. Yang, C. Zhao, P. Zhou, and W. Xu, "MIMO detection of 16-QAM signaling based on semidefinite relaxation," *IEEE Signal Processing Letters*, vol. 14, no. 11, pp. 797–800, Nov. 2007.
- [20] N. D. Sidiropoulos and Z.-Q. Luo, "A semidefinite relaxation approach to MIMO detection for high-order QAM constellations," *IEEE Signal Processing Letters*, vol. 13, no. 9, pp. 525–528, Sep. 2006.
- [21] A. Mobasher, M. Taherzadeh, R. Sotirov, and A. K. Khandani, "A near-maximum-likelihood decoding algorithm for MIMO systems based on semi-definite programming," *IEEE Transactions on Information Theory*, vol. 53, no. 11, pp. 3869–3886, Nov. 2007.
- [22] Z. Mao, X. Wang, and X. Wang, "Semidefinite programming relaxation approach for multiuser detection of QAM signals," *IEEE Transactions on Wireless Communications*, vol. 6, no. 12, pp. 4275–4279, Dec. 2007.
- [23] W.-K. Ma, C.-C. Su, J. Jaldén, T.-H. Chang, and C.-Y. Chi, "The equivalence of semidefinite relaxation MIMO detectors for higher-order QAM," *IEEE Journal of Selected Topics in Signal Processing*, vol. 3, no. 6, pp. 1038–1052, Dec. 2009.
- [24] S. Yang, T. Lv, R. Maunder, and L. Hanzo, "Unified bit-based probabilistic data association aided MIMO detection for high-order QAM constellations," *IEEE Transactions on Vehicular Technology*, vol. 60, no. 3, pp. 981–991, Mar. 2011.
- [25] S. Yang and L. Hanzo, "Semidefinite programming relaxation based virtually antipodal detection for Gray coded 16-QAM MIMO signalling," in *Proc. IEEE Global Telecommunications Conference (GLOBECOM'11)*, Dec. 2011, pp. 1–5.
- [26] J. Hoydis, S. ten Brink, and M. Debbah, "Massive MIMO: How many antennas do we need?" in *Proc. 2011 49th Annual Allerton Conference on Communication, Control, and Computing (Allerton'11)*, Sep. 2011, pp. 545–550.
- [27] L. Hanzo, H. Haas, S. Imre, D. O'Brien, M. Rupp, and L. Gyongyosi, "Wireless myths, realities, and futures: From 3G/4G to optical and quantum wireless," *Proceedings of the IEEE*, vol. 100, no. Special Centennial Issue, pp. 1853–1888, May 2012.
- [28] C. Helmberg, F. Rendl, R. J. Vanderbei, and H. Wolkowicz, "An interior-point method for semidefinite programming," *SIAM Journal on Optimization*, vol. 6, pp. 342–361, 1996.
- [29] B. Steingrimsson, Z.-Q. Luo, and K. M. Wong, "Soft quasi-maximum-likelihood detection for multiple-antenna wireless channels," *IEEE Transactions on Signal Processing*, vol. 51, no. 11, pp. 2710–2719, Nov. 2003.

- [30] M. Nekui, M. Kisialiou, T. Davidson, and Z.-Q. Luo, "Efficient soft-output demodulation of MIMO QPSK via semidefinite relaxation," *IEEE Journal of Selected Topics in Signal Processing*, vol. 5, no. 8, pp. 1426–1437, Dec. 2011.
- [31] M. Nekui and T. Davidson, "A semidefinite relaxation approach to efficient soft demodulation of MIMO 16-QAM," in *Proc. IEEE International Conference on Communications (ICC'09)*, Dresden, Germany, Jun. 2009, pp. 1–6.



Shaoshi Yang (S'09) received the B.Eng. Degree in information engineering from Beijing University of Posts and Telecommunications, Beijing, China, in 2006. He is currently working toward the Ph.D. degree in wireless communications with the School of Electronics and Computer Science, University of Southampton, Southampton, U.K., through scholarships from both the University of Southampton and the China Scholarship Council.

From November 2008 to February 2009, he was an Intern Research Fellow with the Communications

Technology Laboratory, Intel Labs China, Beijing, where he focused on Channel Quality Indicator Channel design for mobile WiMAX (802.16 m). His research interests include multiuser detection/multiple-input multiple-output detection, multicell joint/distributed processing, cooperative communications, green radio, and interference management. He has published in excess of 20 research papers on IEEE journals and conferences.

Shaoshi is a recipient of the PMC-Sierra Telecommunications Technology Scholarship, and a Junior Member of the Isaac Newton Institute for Mathematical Sciences, Cambridge, UK. He is also a TPC member of both the 23rd Annual IEEE International Symposium on Personal, Indoor and Mobile Radio Communications (IEEE PIMRC 2012), and of the 48th Annual IEEE International Conference on Communications (IEEE ICC 2013).



Tiejun Lv (M'08-SM'12) received the M.S. and Ph.D. degrees in electronic engineering from the University of Electronic Science and Technology of China, Chengdu, China, in 1997 and 2000, respectively. From January 2001 to December 2002, he was a Postdoctoral Fellow with Tsinghua University, Beijing, China. From September 2008 to March 2009, he was a Visiting Professor with the Department of Electrical Engineering, Stanford University, Stanford, CA. He is currently a Professor with the School of Information and Communication

Engineering, Beijing University of Posts and Telecommunications. He is the author of more than 100 published technical papers on the physical layer of wireless mobile communications. His current research interests include signal processing, communications theory and networking. Dr. Lv is also a Senior Member of the Chinese Electronics Association. He was the recipient of the "Program for New Century Excellent Talents in University" Award from the Ministry of Education, China, in 2006.



Lajos Hanzo (F'04) received his degree in electronics in 1976 and his doctorate in 1983. In 2004 he was awarded the Doctor of Sciences (DSc) degree by University of Southampton, U.K., and in 2009 he was awarded the honorary doctorate "Doctor Honoris Causa" by the Technical University of Budapest.

During his 36-year career in telecommunications he has held various research and academic posts in Hungary, Germany and the UK. Since 1986 he has been with the School of Electronics and Computer Science, University of Southampton, U.K., where he holds the chair in telecommunications. He has successfully supervised 80 PhD students, co-authored 20 John Wiley/IEEE Press books on mobile radio communications totalling in excess of 10000 pages, published 1300 research entries at IEEE Xplore, acted both as TPC and General Chair of IEEE conferences, presented keynote lectures and has been awarded a number of distinctions. Currently he is directing a 100-strong academic research team, working on a range of research projects in the field of wireless multimedia communications sponsored by industry, the Engineering and Physical Sciences Research Council (EPSRC), U.K., the European IST Programme and the Mobile Virtual Centre of Excellence (VCE), U.K.. He is an enthusiastic supporter of industrial and academic liaison and he offers a range of industrial courses.

Dr. Hanzo is a Fellow of the Royal Academy of Engineering, and the Institution of Engineering and Technology (IET), as well as the European Association for Signal Processing (EURASIP). He is also a Governor of the IEEE VTS. During 2008-2012 he was the Editor-in-Chief of the IEEE Press and a Chaired Professor at Tsinghua University, Beijing. His research is also funded by the European Research Council's Senior Research Fellow Grant. For further information on research in progress and associated publications please refer to <http://www-mobile.ecs.soton.ac.uk>